



# Molecular fingerprinting with bright, broadband infrared frequency combs

HENRY TIMMERS,<sup>1,\*</sup> ABIJITH KOWLIGY,<sup>1,†</sup> ALEX LIND,<sup>1,6,†</sup> FLAVIO C. CRUZ,<sup>1,2</sup> NIMA NADER,<sup>3</sup> MYLES SILFIES,<sup>4</sup> GABRIEL YCAS,<sup>3</sup> THOMAS K. ALLISON,<sup>4</sup> PETER G. SCHUNEMANN,<sup>5</sup> SCOTT B. PAPP,<sup>1,6</sup> AND SCOTT A. DIDDAMS<sup>1,6</sup>

<sup>1</sup>Time and Frequency Division, National Institute of Standards and Technology, 325 Broadway, Boulder, Colorado 80305, USA

<sup>2</sup>Instituto de Física Gleb Wataghin, Universidade Estadual de Campinas, Campinas, SP, 13083-859, Brazil

<sup>3</sup>Applied Physics Division, National Institute of Standards and Technology, 325 Broadway, Boulder, Colorado 80305, USA

<sup>4</sup>Stony Brook University, Stony Brook, New York 11794-3400, USA

<sup>5</sup>BAE Systems, P.O. Box 868 Nashua, New Hampshire 03063, USA

<sup>6</sup>Department of Physics, University of Colorado, 2000 Colorado Ave., Boulder, Colorado 80309, USA

\*Corresponding author: henry.timmers@nist.gov

Received 5 April 2018; revised 11 May 2018; accepted 14 May 2018 (Doc. ID 327668); published 4 June 2018

**Spectroscopy in the molecular fingerprint spectral region (6.7–20  $\mu\text{m}$ ) yields critical information on material structure for physical, chemical, and biological sciences. Despite decades of interest and effort, this portion of the electromagnetic spectrum remains challenging to cover with conventional laser technologies. In this paper, we present a simple and robust method for generating super-octave, optical frequency combs in the fingerprint region through intra-pulse difference frequency generation in an orientation-patterned gallium phosphide crystal. The attainable brightness from this tabletop source reaches the same level achievable by infrared synchrotron radiation with a bandwidth spanning from 4 to 12  $\mu\text{m}$ . We demonstrate the utility of this unique coherent light source for high-precision, dual-frequency-comb spectroscopy of methanol and ethanol vapor. These results highlight the potential of laser frequency combs for a wide range of infrared molecular sensing applications from basic molecular spectroscopy to nanoscopic imaging.** © 2018 Optical Society of America under the terms of the [OSA Open Access Publishing Agreement](#)

**OCIS codes:** (320.7110) Ultrafast nonlinear optics; (190.4410) Nonlinear optics, parametric processes; (300.6340) Spectroscopy, infrared.

<https://doi.org/10.1364/OPTICA.5.000727>

## 1. INTRODUCTION

Infrared molecular spectroscopy is a powerful and ubiquitous technique for measuring the chemical makeup and structure in almost any state of matter. In particular, the inter-atomic degrees of freedom within a molecule or compound lead to series of discrete, vibrational states whose resonances are unique identifiers in the long-wave infrared (LWIR) spectrum spanning the molecular fingerprint region from 6.7 to 20  $\mu\text{m}$  ( $\sim 1500 - 500 \text{ cm}^{-1}$ ). For the past 50 years, Fourier transform infrared spectroscopy (FTIR) [1] using incoherent, thermal light has been a primary tool for determining molecular structure in this spectral region, imparting wide-ranging impact in the physical, chemical, biological, and medical sciences. However, the low brightness of FTIR thermal sources restricts focusability, long-distance propagation, and spectroscopic sensitivity, while the required mechanical delay of FTIR limits the combination of spectral resolution and measurement time. Infrared laser spectroscopy has been pursued over a similar epoch [2,3], but simultaneous spectral coverage of the entire fingerprint region remains limited to radiation only available at infrared synchrotron facilities [4].

Optical frequency comb spectroscopy [5–7] has been introduced in the past decade as a compelling alternative to FTIR

by providing a unique combination of large spectral bandwidth, high frequency precision, and rapid data acquisition that can be integrated with cavity enhancement techniques [8,9] or long-distance propagation [10] to enhance sensitivity. Significant effort has gone into the development and extension of frequency combs deeper into the infrared spectral region beyond 2  $\mu\text{m}$ , with techniques including difference frequency generation (DFG) [11–14], optical parametric oscillation (OPO) [15–17], mode-locked quantum cascade lasers [3], super-continuum generation [18], and Kerr micro-resonator technology [19]. However, to date, most frequency comb sources have been restricted to wavelengths below 6  $\mu\text{m}$  or have only been able to access discrete portions of the fingerprint region with limited resolution and accuracy. In parallel, there has also been ongoing research to generate broadband multi-terahertz pulses extending up to the LWIR region through intra-pulse DFG using mode-locked oscillators based on both Ti:sapphire [5,20,21] and Er:fiber platforms [22,23]. However, reported infrared powers from such optically rectified pulses at  $>10 \text{ MHz}$  repetition rates have been limited to the microwatt ( $\mu\text{W}$ ) scale.

In this paper, we introduce a solution for bright, stabilized LWIR frequency combs based on intra-pulse DFG using a few-cycle pulse derived from commonplace and robust Er:fiber

laser technology. The parametric conversion occurs within a quadratic nonlinear crystal employing quasi-phase matching to enhance the light conversion efficiency into the LWIR regime. In this manner, we generate spectra containing up to 0.25 mW of power and spanning 4–12  $\mu\text{m}$  (2500 – 830  $\text{cm}^{-1}$ ), with a pathway to coverage across the full fingerprint region. The present super-octave bandwidth consists of 500,000 frequency comb modes, providing a spectral resolution down to 100 MHz (0.0033  $\text{cm}^{-1}$ ). We illustrate the capabilities of this unique spectroscopic tool by measuring mode-resolved spectra of methanol and broadband spectra of ethanol molecules using a second comb source for readout in a dual-comb spectroscopy (DCS) configuration [7]. Our results realize improvements in resolution that

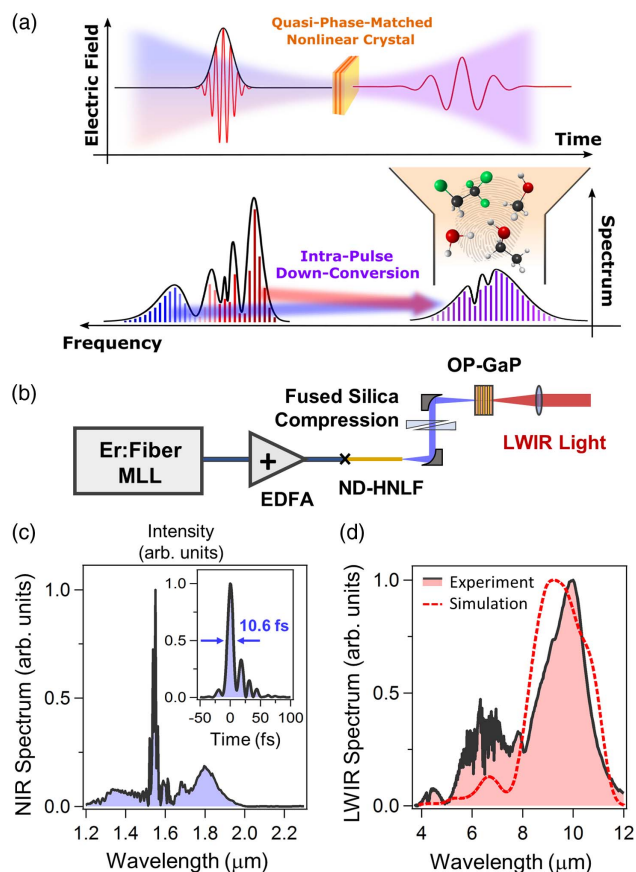


**Fig. 1.** Experimental layout for intra-pulse DFG comb generation. (a) Conceptually, in the time domain (top panel) a few-cycle pulse undergoes intra-pulse DFG within a quasi-phase-matched, nonlinear crystal, leading to the generation of radiation with a longer optical period than the pump pulse. In the frequency domain (bottom panel), the various comb modes within the few-cycle pulse spectrum mix within the crystal, leading to the generation of down-converted light lying within the molecular fingerprint window. (b) Experimentally, the output of a Er mode-locked laser (MLL) is amplified using an Er-doped fiber amplifier (EDFA) and undergoes nonlinear broadening within a normal dispersion highly nonlinear fiber (ND-HNLF). The positive chirp accumulated within the ND-HNLF is compensated for using a pair of fused silica wedges, resulting in a few-cycle pump pulse. The spectrum of this few-cycle driver is shown in (c). The inset of (c) displays the measured intensity profile of the pump pulse, corresponding to a pulse duration of 10.6 fs. (d) When the pump pulse is focused into an OP-GaP crystal, we generate super-octave LWIR spectra containing up to 0.25 mW of power. This spectrum is well reproduced by simulation.

are over a factor of 100 beyond the two previously reported frequency-comb spectroscopy measurements in the fingerprint region [5,24]. Additionally, the frequency axis of the spectra we recover is precisely calibrated with respect to absolute microwave standards at fractional uncertainties below  $1 \times 10^{-11}$ . Finally, the acquisition rate of 20 ms and favorable signal-to-noise ratio allows us to demonstrate dynamic sampling and tracking of gas concentrations on the second time scale.

Of equal significance, with this simple and robust table-top source, we produce coherent, broadband infrared light exhibiting comparable brightness to an infrared beamline at synchrotron user facilities. This opens new possibilities for infrared scanning probe nanoscopy [25,26]. Moreover, the potential for achieving still broader spectral coverage and higher powers should be enabling for a wide range of diagnostics of chemical and biological species, including applications in astronomical heterodyne spectroscopy [27] and nonlinear spectroscopy [6,28].

The concept and implementation of our frequency comb source is depicted in Fig. 1. In the time domain [Fig. 1(a), top panel], a few-cycle pulse is focused into the nonlinear crystal, resulting in a nonlinear polarization and forward emission of LWIR light having an optical period on the order of the temporal duration of the pump pulse. In the frequency domain [Fig. 1(a), lower panel], this corresponds to DFG between the spectral components within the few-cycle, near-infrared pump spectrum. Since the few-cycle pulses occur as a coherent pulse train, the pump spectrum consists of a comb of frequency modes given by  $\nu_n = f_0 + n \times f_{\text{rep}}$ , where  $f_0$  is the carrier-envelope offset frequency and  $f_{\text{rep}}$  is the repetition rate of the pulse train. The pairwise difference between the  $n$ th and  $m$ th pump modes yields a LWIR comb with frequencies  $\nu_i = (n - m) \times f_{\text{rep}}$ . A critical and advantageous aspect of the intra-pulse difference frequency is that  $f_0$  is subtracted out from the pump field, providing a phase-stable, offset-free LWIR comb consisting of exact harmonics of  $f_{\text{rep}}$ .

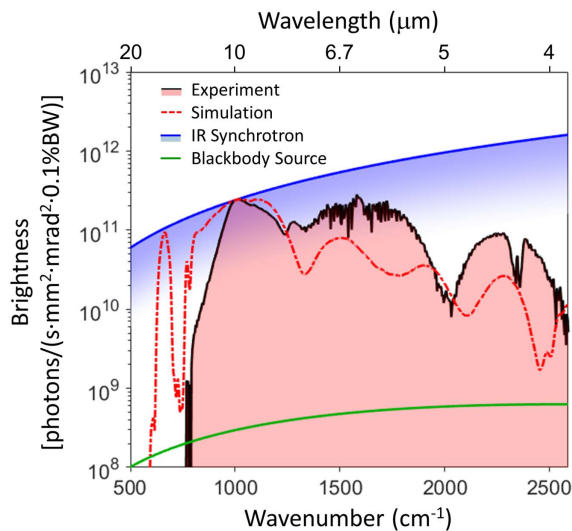


**Fig. 2.** Brightness comparison between broadband infrared sources. The brightness of the experimental and simulated intra-pulse DFG spectrum is plotted in comparison to more conventional broadband infrared sources. This experimental source is significantly brighter than a blackbody lamp and on par with the maximum brightness attainable from a synchrotron infrared user facility.

The experimental layout used to implement the broadband, few-cycle Er comb is shown in Fig. 1(b), with complete experimental details given in Supplement 1. Briefly, femtosecond pulses generated from a 100 MHz Er: fiber mode-locked oscillator are amplified to a pulse energy of 3.5 nJ, corresponding to an average power of 350 mW. The compressed output of the amplifier is spliced directly to a normal dispersion highly nonlinear fiber (ND-HNLF, 4 cm), where the pulse undergoes spectral broadening to generate a bandwidth of  $\sim 600$  nm [Fig. 1(c)]. The positively chirped pulse exiting the HNLF is temporally compressed with anomalous dispersion fused silica wedges and characterized using frequency resolved optical gating (see Supplement 1). The reconstructed pulse profile [inset of Fig. 1(c)] yields a temporal duration of 10.6 fs, corresponding to a two-cycle pulse.

After compression, the few-cycle pulse is focused into an OP-GaP crystal with an orientation patterning period of  $\Lambda = 61.1$   $\mu\text{m}$  and a thickness of 1 mm. The OP-GaP crystal exhibits a high nonlinear coefficient ( $d_{\text{eff}} = 27$  pm/V at 1.3  $\mu\text{m}$ ) and broad transparency across the pump and LWIR wavelength regime [29–31], making it ideally suited for intra-pulse down-conversion. The generated LWIR light is collected after the OP-GaP crystal and long-pass filtered at 3.6  $\mu\text{m}$ . Using this

simple setup, we generate LWIR spectra spanning across both infrared atmospheric transmission bands (3–5  $\mu\text{m}$  and 8–12  $\mu\text{m}$ ) and containing up to 0.25 mW of power. A typical spectrum optimized for bandwidth is shown in Fig. 1(d), exhibiting over 1.5 octaves of bandwidth from 4 to 12  $\mu\text{m}$ . In addition, we plot a simulated LWIR spectrum calculated using a nonlinear envelope equation [32]. The simulated spectrum accounts for the 12  $\mu\text{m}$  spectral cutoff from the HgCdTe (MCT) detectors employed in the experiment.

While there is significant interest in utilizing broadband infrared sources spanning the molecular fingerprint region, only a few options exist with the desirable combination of bandwidth and brightness, including blackbody lamps common in FTIR and broadband radiation derived from synchrotron user facilities [4]. We compare the brightness of our experimental spectrum in Fig. 2 with the calculated brightness of a blackbody lamp and the upper limit for the peak brightness from an infrared synchrotron beamline (500 mA ring current) [33]. The infrared brightness available from these synchrotron beamlines is usually within an order of magnitude from this theoretical upper limit. As can be seen, the OP-GaP source is more than 3 orders of magnitude greater than the blackbody source and on the same order of

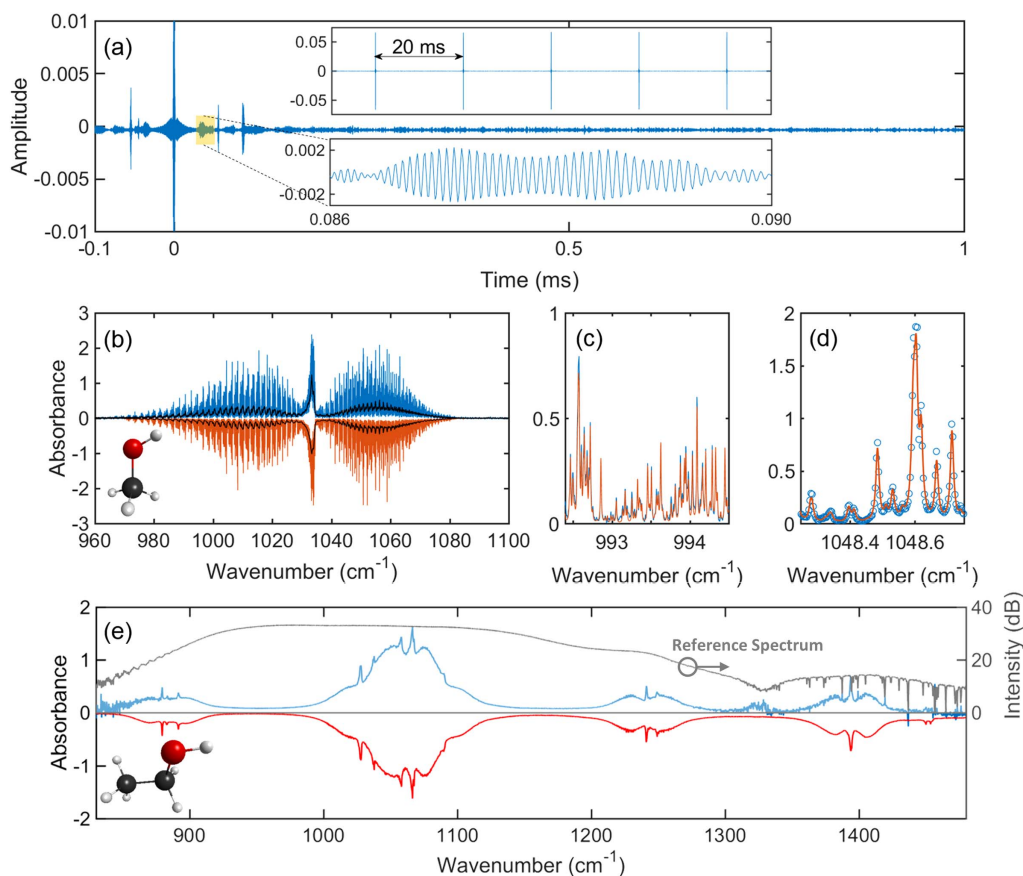


**Fig. 3.** Dual-comb spectroscopy of methanol and ethanol. (a) In the time domain, the multi-heterodyne signal from two LWIR frequency combs results in a periodic interferogram with a recurrence period of  $1/\delta f_{\text{rep}} = 20$  ms. A sequence of 5 interferograms is shown in the inset (top) for the acquisition of comb-tooth resolved spectra. The free-induction decay signature of molecular absorption is shown in the bottom inset, highlighting the high temporal resolution of a complete absorption cycle. (b) The measured DCS absorbance spectrum of methanol at low pressure (blue curve) compared against the methanol spectrum from the HITRAN2012 reference model [34] (red, reflected about origin). The overlaying black curves are the experimental and modeled spectra for methanol acquired at atmospheric pressure. (c) To demonstrate the resolution and agreement, we plot a 2  $\text{cm}^{-1}$  subset of the spectrum around 993.5  $\text{cm}^{-1}$ . (d) The DCS spectrum arising from the phase-coherent acquisition of multiple interferograms resolves the individual 100 MHz comb modes, represented as open circles. (e) We also collect an ethanol DCS spectrum (blue) spanning a 700  $\text{cm}^{-1}$  window around 1050  $\text{cm}^{-1}$  to demonstrate the broadband acquisition capabilities of the LWIR frequency comb. The experimental spectrum agrees well with the PNNL reference model [35].

magnitude compared against the large-scale synchrotron facilities. Further, we plot the brightness of the simulated LWIR spectrum from Fig. 1(d) without the MCT spectral response. The full spectrum extends beyond 15  $\mu\text{m}$ , suggesting its application as a bright table-top alternative to synchrotron infrared radiation.

To demonstrate the utility of our LWIR frequency comb, we perform high-resolution DCS of vapor phase methanol and ethanol. In DCS, a second frequency comb with a slight offset in its repetition rate,  $\delta f_{\text{rep}}$ , is used. The LWIR light from the two combs is combined, passes through a 15 cm molecular absorption cell, and is then photo-detected. The time-dependent interference between the two combs gives rise to a periodic interferogram with a recurrence of  $1/\delta f_{\text{rep}}$ , analogous to FTIR, but generated without the need for meter-scale mechanical delay.

The DCS interferogram measured from methanol vapor is shown in Fig. 3(a). In this experiment, we use a  $\delta f_{\text{rep}} = 50$  Hz and a temporal acquisition window of  $T = 1/\delta f_{\text{rep}} = 20$  ms to achieve a frequency resolution of 100 MHz. Most of the molecular information is contained in the long tails and revivals following the central burst [bottom inset in Fig. 3(a)]. The DCS absorbance spectrum of methanol,  $A(\omega)$ , is presented in Fig. 3(b) and is measured as

$$A(\omega) = -\ln \left[ \frac{|\tilde{I}_A(\omega)|}{|\tilde{I}_o(\omega)|} \right], \quad (1)$$

where  $\tilde{I}_A(\omega)$  and  $\tilde{I}_o(\omega)$  are the DCS spectra with and without an absorption cell, respectively, and a DCS spectrum is calculated by taking a Fourier transform of the interferogram, or  $\tilde{I}(\omega) = \mathcal{F}[I(t)]$ . The spectrum in Fig. 3(b) corresponds to the *P*, *Q*, and *R* branches of the C-O stretch transition in methanol centered at 1033  $\text{cm}^{-1}$  ( $\sim 9.7$   $\mu\text{m}$ ). We collect the methanol absorption spectrum at both atmospheric pressure (methanol partial pressure of  $\sim 3$  mbar, black curve), where the ro-vibrational lines are pressure broadened to  $\sim 10$  GHz, and at a lower background pressure of 50 mbar (methanol partial pressure of 3 mbar, blue curve), where we can resolve sub-gigahertz (GHz) linewidths. These collected spectra are in agreement with the methanol spectra calculated from the HITRAN2012 database [34] (black and red curves reflected about origin, corresponding to spectra at atmospheric pressure and 50 mbar, respectively). To exemplify this agreement, we present a zoom into a subset of data at 993.5  $\text{cm}^{-1}$  in Fig. 3(c). Further, to demonstrate the low phase noise between the two LWIR combs, we additionally collect five interferograms in a 100 ms window and average 5000 recurrences [upper inset of Fig. 3(a)]. With multiple interferograms, we resolve the individual comb teeth, which are indicated by the open-circle markers in Fig. 3(d).

In the data of Fig. 3, we see a measurable disagreement with HITRAN2012. Due to the intrinsic precision of DCS, we do not believe this can arise from calibration error of the frequency axis. On the other hand, the methanol data set used for the HITRAN2012 database was averaged over multiple FTIR acquisitions, exhibiting a variation in absorbance of up to 20%, and the line list was modeled without the inclusion of vibrational interactions [36]. Therefore, the disagreement could arise from the imprecision of the database itself. Techniques such as ours could therefore be invaluable to resolving such issues.

In addition to measuring fine spectral resolution, these super-octave combs can be utilized to resolve broadband absorbers in the molecular fingerprint region. To highlight this, we collect

an ethanol DCS spectrum in Fig. 3(e) (blue curve) spanning a 700  $\text{cm}^{-1}$  window across four broadband features. The measured DCS spectrum is in remarkable agreement with the ethanol reference spectrum (red curve) from the Pacific Northwest National Lab (PNNL) infrared database [35]. Furthermore, by characterizing the noise on the reference spectrum [black curve in 3(e)], we estimate a signal-to-noise ratio of  $\text{SNR} = 14 \text{ Hz}^{1/2}$  for the  $M \sim 10^5$  modes within the central 300  $\text{cm}^{-1}$  spectral width (see Supplement 1). This yields a DCS quality factor [7] of  $M \times \text{SNR} = 1.4 \times 10^6 \text{ Hz}^{1/2}$ , which is unparalleled for the fingerprint region and competitive with other DCS measurements performed at shorter wavelengths.

Due to the good SNR of the LWIR combs, DCS can be performed over fairly short averaging times (see Visualization 1). To demonstrate this, we collect a time series of methanol DCS spectra averaged over 100 interferograms ( $\sim 2$  s averaging time) in Fig. 4(a). We again use  $\delta f_{\text{rep}} = 50$  Hz; however, we reduce the DCS acquisition window to 285  $\mu\text{s}$ , corresponding to a spectral resolution of 7 GHz. In contrast to the static measurements of Fig. 3, here we place a drop of methanol into the open gas cell and record the absorbance spectrum as it evaporates. The total time series window is 350 s, during which we can capture the initial evaporation of the methanol leading to a local increase in its partial pressure as well as the slow diffusion of the vapor into the atmosphere. These dynamics are captured in the average absorbance plot in Fig. 4(b), demonstrating the utility of LWIR DCS in monitoring transient changes in absorption spectra on few-second reaction time scales. Figure 4(c) plots absorbance spectra at various time points depicted by the dashed lines in Fig. 4(a). The distorted line shapes in panel (ii) arise due to saturation of the absorption lines, for which we do not have sufficient dynamic range to accurately

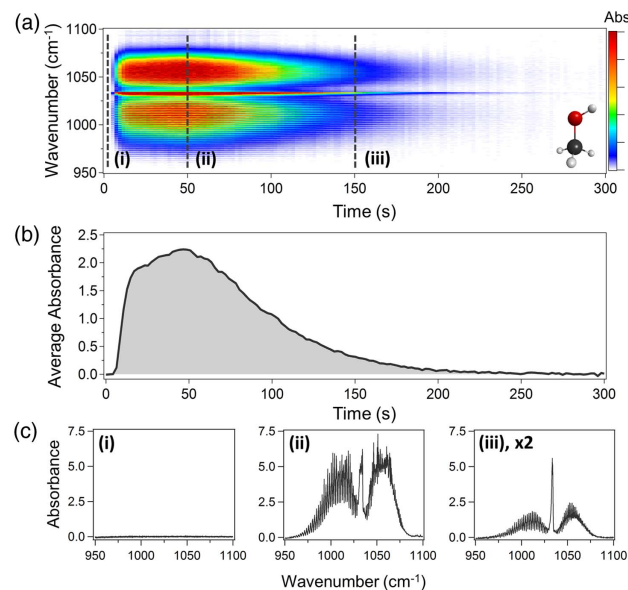


**Fig. 4.** Time-series analysis of methanol evaporation. (a) A time series of DCS spectra collected during the evaporation of methanol within the absorption gas cell. (b) The measured average absorbance demonstrates the ability of LWIR-based DCS in detecting transient changes in a reaction occurring on a few-second time scale. (c) Spectral line outs of the time series taken along the lines denoted by (i), (ii), and (iii) in (a). Even with a short averaging time of 2 s per time step, we can achieve simultaneous high spectral resolution (7 GHz) and high signal-to-noise ratio ( $\text{SNR} = 67 \text{ Hz}^{1/2}$ ).

record. However, despite the fast acquisition time, we can still resolve the narrow ro-vibrational absorption features of methanol with a  $\text{SNR} = 67 \text{ Hz}^{1/2}$  throughout the data set.

In conclusion, we present a powerful scheme for generating super-octave spanning LWIR frequency combs driven by a robust, few-cycle Er-pump infrastructure. The combination of high-resolution and fast-acquisition DCS demonstrates the potential of these low-noise, LWIR combs for a wide range of molecular fingerprint applications, both in lab-based and field-based instruments. In addition, the brightness achieved by these combs offer a competitive alternative to large-scale user facilities. The intra-pulse DFG technique can also be extended to integrated photonics platforms to generate broadband infrared light in a compact footprint [37]. Going forward, we envision optically up-converting the LWIR combs via an electro-optical sampling scheme [21–23,38] to implement LWIR spectroscopy without the need for cryogenically cooled MCT photo-detectors in order to capture and utilize the full LWIR spectrum.

**Funding.** Defense Advanced Research Projects Agency (DARPA); National Institute of Standards and Technology (NIST); National Science Foundation (NSF) (1708743); Air Force Office of Scientific Research (AFOSR) (FA9550-16-1-0016).

**Acknowledgment.** H. Timmers acknowledges support from the National Research Council. M. C. Silfies acknowledges support from the GAANN program of the Dept. of Education. We thank J. Biegert, I. Coddington, F. Giorgetta, D. Hickstein, A. Leitenstorfer, M. Raschke, and N. Newbury for valuable comments and discussions.

See [Supplement 1](#) for supporting content.

<sup>†</sup>These authors contributed equally to this work.

## REFERENCES

- P. Griffiths and J. de Haseth, *Fourier Transform Infrared Spectrometry*, 2nd ed. (Wiley, 2007).
- A. Schliesser, N. Picqué, and T. W. Hänsch, "Mid-infrared frequency combs," *Nat. Photonics* **6**, 440–449 (2012).
- A. Hugi, G. Villares, S. Blaser, H. C. Liu, and J. Faist, "Mid-infrared frequency comb based on a quantum cascade laser," *Nature* **492**, 229–233 (2012).
- P. Roy, M. Rouzières, Z. Qi, and O. Chubar, "The AILES infrared beamline on the third generation synchrotron radiation facility SOLEIL," *Infrared Phys. Technol.* **49**, 139–146 (2006).
- F. Keilmann, C. Gohle, and R. Holzwarth, "Time-domain mid-infrared frequency-comb spectrometer," *Opt. Lett.* **29**, 1542–1544 (2004).
- T. Ideguchi, S. Holzner, B. Bernhardt, G. Guelachvili, N. Picqué, and T. W. Hänsch, "Coherent Raman spectro-imaging with laser frequency combs," *Nature* **502**, 355–358 (2013).
- I. Coddington, N. Newbury, and W. Swann, "Dual-comb spectroscopy," *Optica* **3**, 414–426 (2016).
- B. Bernhardt, A. Ozawa, P. Jacquet, M. Jacquy, Y. Kobayashi, T. Udem, R. Holzwarth, G. Guelachvili, T. W. Hänsch, and N. Picqué, "Cavity-enhanced dual-comb spectroscopy," *Nat. Photonics* **4**, 55–57 (2010).
- B. Spaun, P. B. Changala, D. Patterson, B. J. Bjork, O. H. Heckl, J. M. Doyle, and J. Ye, "Continuous probing of cold complex molecules with infrared frequency comb spectroscopy," *Nature* **533**, 517–520 (2016).
- G. B. Rieker, F. R. Giorgetta, W. C. Swann, J. Köfler, A. M. Zolot, L. C. Sinclair, E. Baumann, C. Cromer, G. Petron, C. Sweeney, P. P. Tans, I. Coddington, and N. R. Newbury, "Frequency-comb-based remote sensing of greenhouse gases over kilometer paths," *Optica* **1**, 290–298 (2014).
- C. Emy, K. Moutzouris, J. Biegert, D. Kühke, F. Adler, A. Leitenstorfer, and U. Keller, "Mid-infrared difference-frequency generation of ultrashort pulses tunable between 3.2 and 4.8  $\mu\text{m}$  from a compact fiber source," *Opt. Lett.* **32**, 1138–1140 (2007).
- F. C. Cruz, D. L. Maser, T. Johnson, G. Ycas, A. Klose, F. R. Giorgetta, I. Coddington, and S. A. Diddams, "Mid-infrared optical frequency combs based on difference frequency generation for molecular spectroscopy," *Opt. Express* **23**, 26814–26824 (2015).
- K. F. Lee, C. J. Hensley, P. G. Schunemann, and M. E. Fermann, "Midinfrared frequency comb by difference frequency of erbium and thulium fiber lasers in orientation-patterned gallium phosphide," *Opt. Express* **25**, 17411–17416 (2017).
- G. Ycas, F. R. Giorgetta, E. Baumann, I. Coddington, D. Herman, S. A. Diddams, and N. R. Newbury, "High-coherence mid-infrared dual-comb spectroscopy spanning 2.6 to 5.2  $\mu\text{m}$ ," *Nat. Photonics* **12**, 202–208 (2018).
- F. Adler, P. Maslowski, A. Foltynowicz, K. C. Cossel, T. C. Briles, I. Hartl, and J. Ye, "Mid-infrared Fourier transform spectroscopy with a broadband frequency comb," *Opt. Express* **18**, 21861–21872 (2010).
- L. Maidment, P. G. Schunemann, and D. T. Reid, "Molecular fingerprint-region spectroscopy from 5 to 12  $\mu\text{m}$  using an orientation-patterned gallium phosphide optical parametric oscillator," *Opt. Lett.* **41**, 4261–4264 (2016).
- A. V. Muraviev, V. O. Smolski, Z. E. Loparo, and K. L. Vodopyanov, "Massively parallel sensing of trace molecules and their isotopologues with broadband subharmonic mid-infrared frequency combs," *Nat. Photonics* **12**, 209–214 (2018).
- N. Nader, D. L. Maser, F. C. Cruz, A. Kowligy, H. Timmers, J. Chiles, C. Fredrick, D. A. Westly, S. W. Nam, R. P. Mirin, J. M. Shainline, and S. Diddams, "Versatile silicon-waveguide supercontinuum for coherent mid-infrared spectroscopy," *APL Photon.* **3**, 036102 (2018).
- M. Yu, Y. Okawachi, A. G. Griffith, M. Lipson, and A. L. Gaeta, "Mode-locked mid-infrared frequency combs in a silicon microresonator," *Optica* **3**, 854–860 (2016).
- A. Bonvalet, M. Joffre, J. L. Martin, and A. Migus, "Generation of ultra-broadband femtosecond pulses in the mid-infrared by optical rectification of 15 fs light pulses at 100 MHz repetition rate," *Appl. Phys. Lett.* **67**, 2907–2909 (1995).
- R. Huber, A. Brodschelm, F. Tauser, and A. Leitenstorfer, "Generation and field-resolved detection of femtosecond electromagnetic pulses tunable up to 41 THz," *Appl. Phys. Lett.* **76**, 3191–3193 (2000).
- C. Riek, D. V. Seletskiy, A. S. Moskalenko, J. F. Schmidt, P. Krauspe, S. Eckart, S. Eggert, G. Burkard, and A. Leitenstorfer, "Direct sampling of electric-field vacuum fluctuations," *Science* **350**, 420–423 (2015).
- C. Riek, P. Sulzer, M. Seeger, A. S. Moskalenko, G. Burkard, D. V. Seletskiy, and A. Leitenstorfer, "Subcycle quantum electrodynamics," *Nature* **541**, 376–379 (2017).
- O. Kara, L. Maidment, T. Gardiner, P. G. Schunemann, and D. T. Reid, "Dual-comb spectroscopy in the spectral fingerprint region using OPGaP optical parametric oscillators," *Opt. Express* **25**, 32713–32721 (2017).
- B. Pollard, F. C. B. Maia, M. B. Raschke, and R. O. Freitas, "Infrared vibrational nanospectroscopy by self-referenced interferometry," *Nano Lett.* **16**, 55–61 (2015).
- A. Dazzi and C. B. Prater, "AFM-IR: technology and applications in nano-scale infrared spectroscopy and chemical imaging," *Chem. Rev.* **117**, 5146–5173 (2017).
- D. D. S. Hale, M. Bester, W. C. Danchi, W. Fitelson, S. Hoss, E. A. Lipman, J. D. Monnier, P. G. Tuthill, and C. H. Townes, "The Berkeley infrared spatial interferometer: a heterodyne stellar interferometer for the mid-infrared," *Astrophys. J.* **537**, 998–1012 (2000).
- M. A. R. Reber, Y. Chen, and T. K. Allison, "Cavity-enhanced ultrafast spectroscopy: ultrafast meets ultrasensitive," *Optica* **3**, 311–317 (2016).
- I. Shoji, T. Kondo, A. Kitamoto, M. Shirane, and R. Ito, "Absolute scale of second-order nonlinear-optical coefficients," *J. Opt. Soc. Am. B* **14**, 2268–2294 (1997).
- S. Guha, J. O. Barnes, and P. G. Schunemann, "Mid-wave infrared generation by difference frequency mixing of continuous wave lasers in orientation-patterned gallium phosphide," *Opt. Mater. Express* **5**, 2911–2923 (2015).
- P. G. Schunemann, K. T. Zawilski, L. A. Pomeranz, D. J. Creeden, and P. A. Budni, "Advances in nonlinear optical crystals for mid-infrared coherent sources," *J. Opt. Soc. Am. B* **33**, D36–D43 (2016).

32. M. Conforti, F. Baronio, and C. D. Angelis, "Nonlinear envelope equation for broadband optical pulses in quadratic media," *Phys. Rev. A* **81**, 053841 (2010).
33. R. A. Bosch, "Computed flux and brightness of infrared edge and synchrotron radiation," *Nucl. Instrum. Methods Phys. Res. Sect. A* **454**, 497–505 (2000).
34. L. S. Rothman, I. E. Gordon, Y. Babikov, A. Barbe, D. C. Benner, P. F. Bernath, M. Birk, L. Bizzocchi, V. Boudon, L. R. Brown, A. Campargue, K. Chance, E. A. Cohen, L. H. Coudert, V. M. Devi, B. J. Drouin, A. Fayt, J.-M. Flaud, R. R. Gamache, J. J. Harrison, J.-M. Hartmann, C. Hill, J. T. Hodges, D. Jacquemart, A. Jolly, J. Lamouroux, R. J. LeRoy, G. Li, D. A. Long, O. M. Lyulin, C. J. Mackie, S. T. Massie, S. Mikhailenko, H. S. P. Müller, O. V. Naumenko, A. V. Nikitin, J. Orphal, V. Perevalov, A. Perrin, E. R. Polovtseva, C. Richard, M. A. H. Smith, E. Starikova, K. Sung, S. Tashkun, J. Tennyson, G. C. Toon, V. G. Tyuterev, and G. Wagner, "The HITRAN2012 molecular spectroscopic database," *J. Quant. Spectrosc. Radiat. Transfer* **130**, 4–50 (2013).
35. S. W. Sharpe, T. J. Johnson, R. L. Sams, P. M. Chu, G. C. Rhoderick, and P. A. Johnson, "Gas-phase databases for quantitative infrared spectroscopy," *Appl. Spectrosc.* **58**, 1452–1461 (2004).
36. J. J. Harrison, N. D. C. Allen, and P. F. Bernath, "Infrared absorption cross sections for methanol," *J. Quant. Spectrosc. Radiat. Transfer* **113**, 2189–2196 (2012).
37. A. S. Kowligy, A. Lind, D. D. Hickstein, D. R. Carlson, H. Timmers, N. Nader, F. C. Cruz, G. Ycas, S. B. Papp, and S. A. Diddams, "Mid-infrared frequency comb generation via cascaded quadratic nonlinearities in quasi-phase-matched waveguides," *Opt. Lett.* **43**, 1678–1681 (2018).
38. I. Pupeza, D. Sanchez, J. Zhang, N. Lilienfein, M. Seidel, N. Karpowicz, T. Paasch-Colberg, I. Znakovskaya, M. Pescher, W. Schweinberger, V. Pervak, E. Fill, O. Pronin, Z. Wei, F. Krausz, A. Apolonski, and J. Biegert, "High-power sub-two-cycle mid-infrared pulses at 100 MHz repetition rate," *Nat. Photonics* **9**, 721–724 (2015).